ELSEVIER

Journal of Alloys and Compounds 404–406 (2005) 529–532

Journal of ALLOYS AND COMPOUNDS

www.elsevier.com/locate/jallcom

Hydrogenation properties of $Mg/Mg_2Ni_{0.8}Cr_{0.2}$ composites containing TiO_2 nanoparticles

X.L. Wang, J.P. Tu*, X.B. Zhang, C.P. Chen, X.B. Zhao

Department of Materials Science and Engineering, Zhejiang University, Hangzhou 310027, China

Received 25 June 2004; received in revised form 2 September 2004; accepted 6 October 2004
Available online 1 August 2005

Abstract

Mg and Mg-Ni-based hydrides were mechanically milled with TiO_2 nanoparticles to fabricate Mg-*x* wt.% $Mg_2Ni_{0.8}Cr_{0.2}$-1.5 wt.% TiO_2 composites. Due to the combined catalyst effects of the TiO_2 nanoparticles, $Mg_2Ni_{0.8}Cr_{0.2}$ alloy, precipitated Ni particles and the mechanical driving force, the composites showed rapid hydrogen absorption/desorption kinetics. If the content of $Mg_2Ni_{0.8}Cr_{0.2}$ alloy was 20 wt.%, the composite could absorb 4.6 wt.% H at 373 K within 3 min and desorb 4.19 wt.% H at 513 K within 50 min.

Keywords: Hydrogen storage; Mg-based composite; Hydriding/dehydriding kinetics; Ball milling; Catalyst

1. Introduction

Owing to the high hydrogen storage capacity per unit weight, Mg-based alloys have attracted extensive attention for several decades [1–3]. Unfortunately, their hydrides are too stable for most practical applications. Therefore, to destabilize their hydrides and to improve their hydriding-dehydriding kinetics are appealing objectives. Modifying the hydriding properties of pure Mg by incorporating it into some materials having lower stability is an efficient method, and the corresponding materials are referred to as Mg-based composites.

However, the high ductility of Mg metal impedes a high-degree dispersion of the catalytic phase that further restricts the full realization of the catalytic function. This problem could be overcome successfully by milling brittle Mg hydride instead of Mg metal. Recently, transition metal oxides have been used as catalyst for the Mg-based hydrogen storage alloys [4–7]. The oxides are hard and brittle and may therefore promote a better dispersion of Mg particles. If the content of TiO_2 was 1.5 wt.%, the $Mg_2Ni_{0.75}Cr_{0.25}/TiO_2$ nanocomposite could absorb 2.2 wt.% hydrogen under 4 MPa H_2 at 373 K [6]. In this work, the effect of both $Mg_2Ni_{0.8}Cr_{0.2}$ alloy and TiO_2 nanoparticles on absorption and desorption properties of Mg was investigated.

2. Experimental details

The magnesium, nickel and chromium powder (purity 99.9%, 200 mesh), corresponding to an atomic proportion of 2:0.8:0.2 were mechanically mixed under argon in a planetary ball mill machine for 1 h. After the milling, the mixture was cold pressed into pellets under a pressure of 800 MPa and sintered at 823 K for 3 h in argon atmosphere. The pellets of $Mg_2Ni_{0.8}Cr_{0.2}$ were pulverized to particles smaller than 100 mesh. Then mixtures composed of magnesium powder, 1.5 wt.% TiO_2 nanoparticles (tetragonal structure, average size 40 nm) and the $Mg_2Ni_{0.8}Cr_{0.2}$ powder taken in different proportions of 20, 25, 30 and 50 wt.% were ball-milled for 1 h. After milling, the mixtures were activated at 613 K at 4.0 MPa H_2 for 8 h. Thereafter, the multi-phase hydrides were ball-milled for 50 h under argon with a ball-to-powder weight ratio of 20:1. Microstructure and morphology of the samples were examined by XRD (Philips PW1050 diffractometer, Cu Kα radiation) and SEM (FEI, SIRION).

The apparatus for hydriding/dehydriding measurements are similar to the equipment described in [8]. The vessel filled with a 3.0 g powder sample was evacuated to 10^{-2} Pa by

* Corresponding author. Tel.: +86 571 87952573; fax: +86 571 87952573.
E-mail address: tujp@cmsce.zju.edu.cn (J.P. Tu).

0925-8388/$ – see front matter © 2005 Elsevier B.V. All rights reserved.
doi:10.1016/j.jallcom.2004.10.097

a rotary vacuum pump and heated to 573 K for 1 h. Then the temperature was set equal to 353 K, and hydrogen was introduced at an initial pressure of 4 MPa. After measuring the hydrogen absorbing behavior at 353 K, the vessel was evacuated to 0.1 MPa and heated to above 513 K to desorb the hydrogen.

3. Results and discussion

3.1. Microstructural characterization

Fig. 1 shows the X-ray diffraction patterns of Mg-x wt.% $Mg_2Ni_{0.8}Cr_{0.2}$ ($x = 20, 25, 30, 50$) hydrides with 1.5 wt.% TiO_2 nanoparticles after ball milling for 50 h. It can be seen that the diffraction peaks are broadened and the intensity decreases significantly. This indicates the grain refining and the introduction of strain into the samples. MgH_2 and Mg_2NiH_4 were the main phases in the X-ray diffraction patterns. Some Mg_2NiH and pure Mg were also present because the hydrides were not stable and partly decomposed during the ball milling. Pure Ni was also formed because the $Mg_2Ni_{0.8}Cr_{0.2}$ alloy was unstable towards the substitution of Cr atoms and Ni precipitated onto the surface of the particles. Additionally, the diffraction peaks became broader and the intensity of the Ni peaks increased with the increase of the $Mg_2Ni_{0.8}Cr_{0.2}$ alloy content.

The SEM micrographs of as-milled Mg-x wt.% $Mg_2Ni_{0.8}Cr_{0.2}$ composites are presented in Fig. 2. As can be easily seen, the particle size decreases with increasing content of the $Mg_2Ni_{0.8}Cr_{0.2}$ alloy that agrees with the XRD results. The particles were irregular because there were more than one phase formed during ball milling and hydrides were brittle and easily crushed. The full realization of the catalyst function depends not only on the catalytic characteristics of the composite phase, but also on its distribution state [9]. The EDS spectrum of Ti metal in the Mg-20 wt.% $Mg_2Ni_{0.8}Cr_{0.2}$-1.5 wt.% TiO_2 composite (sample A) shows that TiO_2 nanoparticles disperse uniformly in the composite. The EDS spectrum of Ti metal in other three samples is similar.

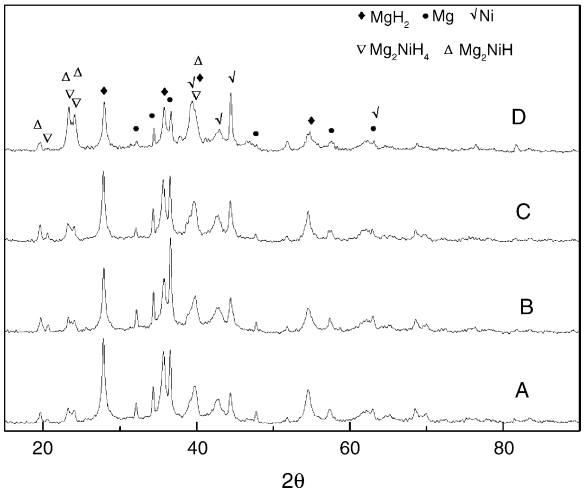

Fig. 1. X-ray diffraction patterns of hydrides of Mg-x wt.% $Mg_2Ni_{0.8}Cr_{0.2}$-1.5 wt.% TiO_2 composites after ball milling for 50 h; $x = 20$ (A), 25 (B), 30 (C) and 50 (D).

3.2. Hydrogenation properties

It was found that hydrogenation capacities are closely correlated with the microstructures and the types of phases present in the composite materials. After being dehydrided at 573 K, the as-milled samples needed no activation for

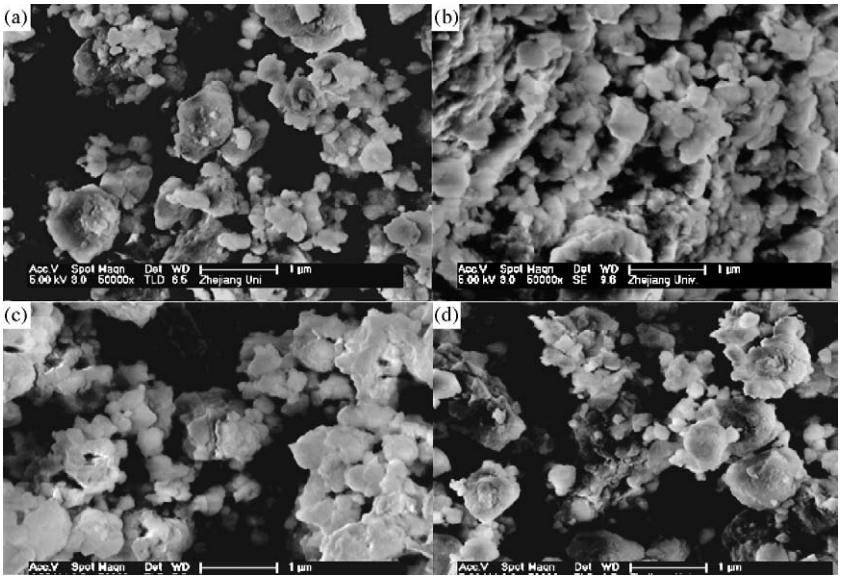

Fig. 2. Field emission SEM image of hydrides of Mg-x wt.% $Mg_2Ni_{0.8}Cr_{0.2}$-1.5 wt.% TiO_2 composites after ball milling for 50 h; $x = 20$ (a), 25 (b), 30 (c) and 50 (d).

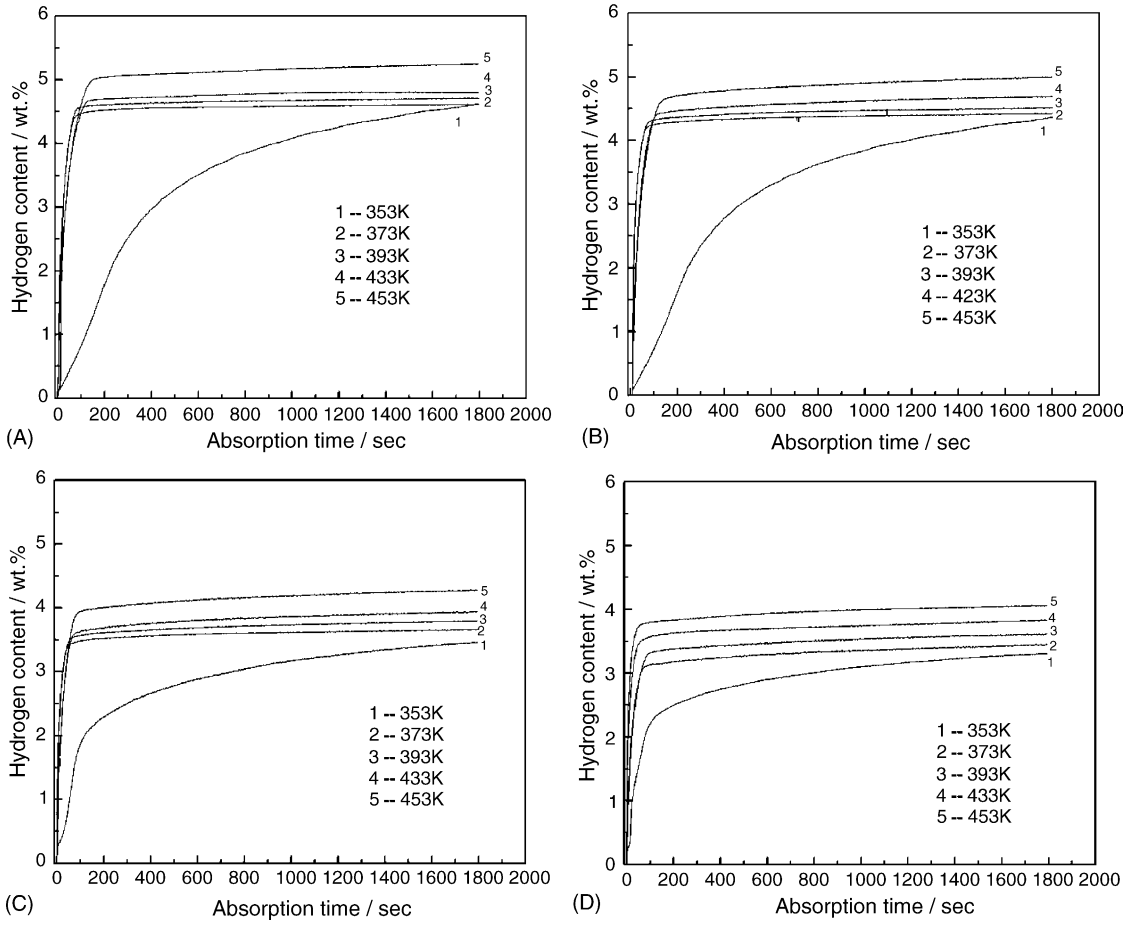

Fig. 3. Hydrogen absorption kinetics of Mg-x wt.% $Mg_2Ni_{0.8}Cr_{0.2}$-1.5 wt.% TiO_2 composites at different temperatures; $x = 20$ (A), 25 (B), 30 (C) and 50 (D).

rapid H-absorption. From the hydriding behavior of the Mg-x wt.% $Mg_2Ni_{0.8}Cr_{0.2}$-1.5 wt.% TiO_2 composites at different temperatures under an initial hydrogen pressure of 4.0 MPa (shown in Fig. 3), it can be seen that all the composites possessed a superior kinetics at temperatures exceeding 373 K. With increasing absorption temperature, the maximum hydrogen content increases. Fig. 4 shows the hydrogen absorption kinetics of the Mg-x wt.% $Mg_2Ni_{0.8}Cr_{0.2}$-1.5 wt.% TiO_2 composites at 373 K. It indicates that composite has lower H-absorption rates compared with other three samples. The H-absorption capacity was 4.60, 4.42, 3.65 and 3.44 wt.% H for $x = 20$, 25, 30 and 50, respectively. It may also be noted that all the absorption was within 3 min.

To further investigate the hydriding characteristics of the composites at low temperatures, H-absorption measurements were carried out at 353 K. As seen from Fig. 3, the maximum hydrogen content decreased with increasing content of the $Mg_2Ni_{0.8}Cr_{0.2}$ alloy and was equal to 5.24, 4.99, 4.27 and 4.05 wt.% H for $x = 20$, 25, 30, and 50, respectively. However, all the composites show relatively low hydriding rates at 353 K.

On the desorption side, the composites also exhibited rather high rates. Fig. 5 presents the hydrogen desorption curves of the Mg-x wt.% $Mg_2Ni_{0.8}Cr_{0.2}$-1.5 wt.% TiO_2 composites under 0.1 MPa at 513 K. As shown in Fig. 5, 4.2 wt.% H_2 is released in 48 min. With increasing content of $Mg_2Ni_{0.8}Cr_{0.2}$, the maximum desorbed hydrogen content decreases and the desorption kinetics improves. From the above results, it can be concluded that adding 20 wt.%

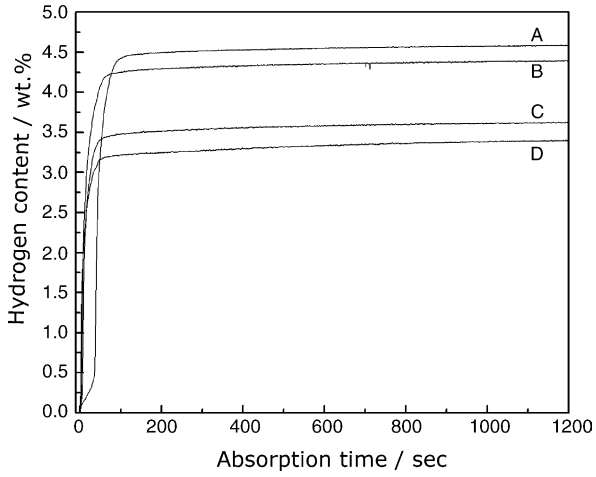

Fig. 4. Hydrogen absorption kinetics of Mg-x wt.% $Mg_2Ni_{0.8}Cr_{0.2}$-1.5 wt.% TiO_2 composites at 373 K; $x = 20$ (A), 25 (B), 30 (C) and 50 (D).

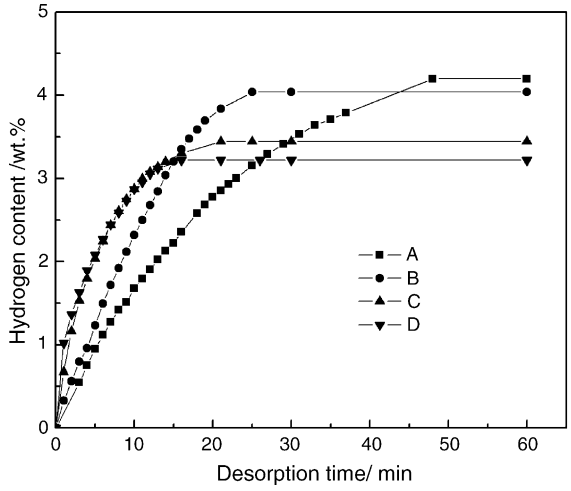

Fig. 5. Hydrogen desorption kinetics of Mg-based composites at 513 K. A-Mg-20 wt.% $Mg_2Ni_{0.8}Cr_{0.2}$-1.5 wt.% TiO_2; B-Mg-25 wt.% $Mg_2Ni_{0.8}Cr_{0.2}$-1.5 wt.% TiO_2; C-Mg-30 wt.% $Mg_2Ni_{0.8}Cr_{0.2}$-1.5 wt.% TiO_2; D-Mg-50 wt.% $Mg_2Ni_{0.8}Cr_{0.2}$-1.5 wt.% TiO_2.

$Mg_2Ni_{0.8}Cr_{0.2}$ alloy is optimum for the Mg-$Mg_2Ni_{0.8}Cr_{0.2}$-TiO_2 composites. Adding more $Mg_2Ni_{0.8}Cr_{0.2}$ alloy could improve the hydriding/dehydriding kinetics to some extent, but the total hydrogen capacities of the composites was reduced.

The improvement of the absorption/desorption kinetics was attributed to the catalytic effect of both $Mg_2Ni_{0.8}Cr_{0.2}$ alloy and TiO_2 nanoparticles. The hydriding and dehydriding reactions of Mg are nucleation-controlled processes and proceed by the mechanism of nucleation and growth, and the hydriding rates of Mg are controlled by diffusion of hydrogen through the growing layer of Mg hydride. The $Mg_2Ni_{1-X}Cr_X$ alloy can absorb hydrogen at relatively low temperatures and its hydriding is an exothermic process [6]. The exothermic reaction offers energy for the hydrogen absorption by Mg to a certain extent. Therefore, the $Mg_2Ni_{0.8}Cr_{0.2}$ alloy in the composites can act as H diffusion channels with low activation energy. Moreover, the interface between Mg and Mg-Ni acts as an active nucleation site for MgH_2. Zaluska et al. [9] pointed out that the efficiency of the catalyst depended critically on how well it was dispersed through the system. And for this reason the best efficiency of a solid-state catalyst is obtained when the catalyst particles are as small as possible. In the present work, nano-structured TiO_2 acting as catalyst for the hydriding/dehydriding process shows a homogenous dispersion in the composites (see Fig. 2(e)). Furthermore, mechanical milling can facilitate nucleation by creating many defects on the surface and/or in the interior of Mg, or by an additive acting as active sites for the nucleation, and shorten the diffusion distance by reducing the effective particle sizes of Mg. It is reported [10] that nickel particles inlaid on the surface of a nanocrystalline Mg alloy may also act as active sites for the redox reaction of hydrogen and, at the same time, have the "bypass effect" for hydrogen diffusion. Ni precipitated from Mg-Ni alloy can also accelerate the hydrogen diffusion. All the above resulted in the good absorption /desorption kinetics of the composites.

4. Conclusion

Mg and Mg-Ni-based hydrides were mechanically milled with TiO_2 nanoparticles to fabricate Mg-x wt.% $Mg_2Ni_{0.8}Cr_{0.2}$-1.5 wt.% TiO_2 ($x = 20, 25, 30, 50$) composites for hydrogen storage. The hydrides partly decomposed and a small amount of pure Ni precipitated onto the surface of the particles during ball milling. Nanoparticles of TiO_2 produced significant catalytic effects on the hydrogenation properties of the composites due to the homogenous distribution. All the composites can readily absorb hydrogen at 353 K. The composite containing 20 wt.% $Mg_2Ni_{0.8}Cr_{0.2}$ can desorb 4.19 wt.% H at 513 K within 48 min under 0.1 MPa. With increasing content of $Mg_2Ni_{0.8}Cr_{0.2}$, the maximum desorbed hydrogen content decreases while the desorption kinetics improves.

Acknowledgement

This work was supported by the Special Funds for Major States Basic Research Project (no. TG20000264-06) of MOST, China.

References

[1] J.J. Reilly, R.H. Wiswall, Inorg. Chem. 7 (1968) 2254.
[2] H.Y. Shao, H.R. Xu, Y.T. Wang, X.G. Li, Nanotechnology 15 (2004) 269.
[3] A.S. Pedersen, B. Larsen, Int. J. Hydrogen Energy 18 (1993) 297.
[4] W. Oelerich, T. Klassen, R. Bormann, J. Alloys Comp. 315 (2001) 237.
[5] P. Wang, A.M. Wang, H.F. Zhang, B.Z. Ding, Z.Q. Hu, J. Alloys Comp. 313 (2000) 218.
[6] R.G. Gao, J.P. Tu, X.L. Wang, X.B. Zhang, C.P. Chen, J. Alloys Comp. 356–357 (2003) 649.
[7] M.Y. Song, J.L. Bobet, B. Darriet, J. Alloys Comp. 340 (2002) 256.
[8] B. Bogdanović, K. Bohmhammel, B. Christ, A. Reiser, K. Schlichte, R. Vehlen, U. Wolf, J. Alloys Comp. 282 (1999) 84.
[9] A. Zaluska, L. Zaluski, J.O. Ström-Olsen, Appl. Phys. A72 (2001) 157.
[10] N. Cui, P. He, J.L. Luo, Electrochim. Acta 44 (1999) 3549.